

# Wind Tunnel Wall Influence Considering Two-Dimensional High-Lift Configurations

T. E. Labrujère,\* R. A. Maarsingh,\* and J. Smith\*

*National Aerospace Laboratory (NLR), Amsterdam, The Netherlands*

Two alternative correction methods are described for wall interference based on measured boundary conditions. In both methods it is assumed that at or near the tunnel boundary the flow velocity will be measured in magnitude and direction and the main part of the flowfield may be considered irrotational and subsonic. One method aims at a correction in terms of changes in freestream velocity and angle of attack; the other at corrections of the velocity distribution along the model. The application of both methods is demonstrated numerically for single- and multiple-airfoil cases in a solid wall test section.

## Nomenclature

$c$	= airfoil chord
$C_p, C_p$	= lift and pressure coefficients, respectively
$D$	= flow domain
$H$	= tunnel height
$n$	= normal to the flow boundary (directed inward)
$Q$	= dynamic pressure
$r$	= distance between two points $(x,y)$ and $(\xi,\eta)$
$s,t$	= arc length measured along the flow boundary
$u,v$	= disturbance velocity components in $x$ and $y$ directions, respectively
$U,V$	= velocity components in $x$ and $y$ directions, respectively
$x,y$	= Cartesian axis system
$\alpha$	= angle of attack
$\Delta$	= difference
$\xi,\eta$	= integration variables corresponding to $x$ and $y$ , respectively
$\sigma$	= boundary of flow domain
$\varphi$	= disturbance velocity potential
$\phi$	= velocity potential

## Subscripts

$C$	= correction
$F$	= free air
$i$	= reference point for determination of global wall influence
$m$	= mid chord
$M$	= model
$ref$	= undisturbed tunnel flow
$T$	= tunnel
$W$	= walls
$\infty$	= undisturbed free flow

## Introduction

MODERN developments in wind tunnel wall correction methods increasingly have shown the use of methods based on measured boundary conditions. A fairly simple and fast calculation method can be formulated<sup>1</sup> if it is assumed

that the velocity distribution along the tunnel walls can be measured. In principle, this method is applicable to experiments in subsonic and transonic flow, solid and ventilated wall wind tunnels, two-dimensional as well as three dimensional.

From the velocity distribution along the walls, the wall-induced perturbation velocity field can be determined under certain conditions by applying Green's theorem. If the gradients of this perturbation field are small, the wind tunnel influence can be determined in terms of a correction to the freestream velocity and angle of attack. In general, these gradients will be small if the wind tunnel model has a moderate size with respect to the dimensions of the wind tunnel (e.g., in two dimensions for small values of  $c/H$ ). Thus, assuming that in the near future measurement techniques will be improved such that the velocity distribution along the tunnel walls can be measured, it will be possible to determine a sufficiently accurate correction for the majority of wind tunnel experiments.

However, situations may occur where the flow must be considered uncorrectable in this way (e.g., the case of airfoils with high-lift devices at large angles of attack). Having met this difficulty, a limited numerical study of the latter case has been made. It appears that the "uncorrectability" is due to the phenomenon of streamline curvature. The latter is taken into account in a very limited way only when applying a global correction method. This fact has been demonstrated with the aid of an inverse calculation method<sup>2</sup> capable of determining the shape of a multielement airfoil which produces a specified pressure distribution.

From this study it has been concluded that for the flows considered here, correction for wind tunnel wall influence would be feasible only if a local correction method could be developed.

Kraft and Dahm<sup>3</sup> have described an approach that may be used to derive such a method. Their method has the drawback that the airfoil is assumed to be thin and at a low angle of attack, such that a linearized perturbation approximation is valid. But this assumption allows the derivation of closed expressions for local correction in which the model geometry does not appear. As this assumption cannot be made for the flow considered here, the approach of Kraft and Dahm had to be reformulated. This appeared to be possible, though at the cost of introducing a model representation again.

The present paper gives a description of both global and local correction methods. The application of the methods is demonstrated numerically for single- and multiple-airfoil cases in a solid wall test section.

Received May 19, 1985; revision received Sept. 9, 1985. Copyright © American Institute of Aeronautics and Astronautics, Inc., 1985. All rights reserved.

\*Senior Research Engineer, Fluid Dynamics.

## Correction Methods Using Measured Boundary Conditions

### Flow Problem

The correction methods presented herein are both based on the assumption that, at or near the tunnel boundary, the flow velocity will be measured both in magnitude and direction. In the case of solid walls, measurement of the static pressure suffices to determine magnitude and direction, however, in the case of ventilated walls, the flow direction will have to be measured explicitly.

The key problem to be solved when considering wall influence is how to establish a relation between tunnel flow and free flow around a given model. Rather simple solutions to this problem can be formulated if it may be assumed that the flow or at least the greater part of the flow is irrotational and subsonic. With this assumption Goethert's rule may be applied in order to arrive at an equivalent incompressible flow problem. Then the wall influence problem reduces to the problem of relating the incompressible velocity potential  $\phi_T$  of the flow in the tunnel to the incompressible velocity  $\phi_F$  of free flow.

To solve this problem, the flow situations as depicted in Fig. 1 are compared. The velocity potential in the tunnel is split into  $\phi_{ref}$  due to undisturbed flow and  $\phi_T$  due to the disturbance by the tunnel walls and the model. The potential of free flow is split into  $\phi_\infty$  due to undisturbed flow and  $\phi_F$  due to the disturbance by the model. Infinite space is split into three domains: domain  $D_0$  outside the tunnel walls, domain  $D_T$  limited by  $\sigma_W$  at the outer side and  $\sigma_M$  at the inner side, and domain  $D_M$  inside  $\sigma_M$ .

Both of the present methods are based on application of Green's theorem. If the flow in domain  $D$  has cyclic velocity potential  $\phi$ , and  $r$  denotes the distance from any point in the flow domain to a fixed point  $P$ , it can be shown that

$$\int_{\sigma_1 + \sigma_2} \left\{ \phi \frac{\partial}{\partial n} \ln r - \frac{\partial \phi}{\partial n} \ln r \right\} ds + \Delta \phi \int_{\sigma_3} \frac{\partial}{\partial n} \ln r ds = \begin{cases} 0 & \text{for } P \text{ outside } D \\ -\pi \phi(P) & \text{for } P \text{ on the boundary} \\ -2\pi \phi(P) & \text{for } P \text{ inside } D \end{cases} \quad (1)$$

where  $\sigma_1$  and  $\sigma_2$  form the boundary of the flow domain,  $\sigma_3$  is the slit necessary to allow a cyclic potential, and  $\Delta \phi$  the jump in potential across the slit (see Fig. 2).

### Global Correction Method

The global correction method,<sup>1</sup> following the approach as formulated by Ashill and Weeks,<sup>4</sup> aims at the determination of corrections for tunnel wall influence in terms of changes in freestream velocity and angle of attack. The assumption of irrotational subsonic flow is made for a region outside of a relatively small area around the model. Thus, the boundary  $\sigma_M$  in Fig. 1 does not necessarily coincide with the boundary of the model.

In order to be able to determine global corrections it is necessary to assume that, corresponding to the tunnel flow, there exists a free flow around the model such that the disturbances at  $\sigma_M$  in free flow and tunnel flow are approximately the same, and that the lift in both flow situations is the same. Furthermore, it is assumed that the flowfield near the model in the tunnel is globally the same as in free air, such that the velocity will be the same, at least at one suitably chosen point.

For convenience, the present method will be formulated in terms of velocity components rather than velocity potential. Considering domain  $D_T$  (Fig. 1), applying Eq. (1) to  $U = \partial \phi / \partial x$  instead of  $\phi$  and being mindful that this function is single-valued throughout  $D_T$  so that there is no jump in  $U$

across  $\sigma_{ST}$ , the velocity component

$$U_T = U_{ref} + u_T \quad (2)$$

can be determined from

$$U_T = U_{ref} - \frac{1}{2\pi} \int_{\sigma_W} \left\{ u_T \frac{\partial}{\partial n} \ln r - \frac{\partial u_T}{\partial n} \ln r \right\} ds - \frac{1}{2\pi} \int_{\sigma_M} \left\{ u_T \frac{\partial}{\partial n} \ln r - \frac{\partial u_T}{\partial n} \ln r \right\} ds \quad (3)$$

for any point in  $D_T$ . Applying the conditions of continuity and irrotational flow, using partial integration this expression can be rewritten as

$$U_T = U_{ref} - \frac{1}{2\pi} \int_{\sigma_W} \left\{ u_T \frac{\partial}{\partial n} \ln r + v_T \frac{\partial}{\partial s} \ln r \right\} ds - \frac{1}{2\pi} \int_{\sigma_M} \left\{ u_T \frac{\partial}{\partial n} \ln r + v_T \frac{\partial}{\partial s} \ln r \right\} ds \quad (4)$$

In free flow the velocity component

$$U_F = U_\infty + u_F \quad (5)$$

can be determined analogously from

$$U_F = U_\infty - \frac{1}{2\pi} \int_{\sigma_M} \left\{ u_F \frac{\partial}{\partial n} \ln r + v_F \frac{\partial}{\partial s} \ln r \right\} ds \quad (6)$$

As has been stated previously it is assumed that

$$u_F \approx u_T \quad \text{and} \quad v_F \approx v_T \quad \text{at} \quad \sigma_M \quad (7)$$

Hence the second integral of Eq. (4) is approximately equal to the integral of Eq. (6). Furthermore, it is assumed that

$$U_F = U_T \quad \text{at some point in } D_T \quad (8)$$

Thus, from Eqs. (4) and (6), it follows that

$$U_\infty - U_{ref} = -\frac{1}{2\pi} \int_{\sigma_W} \left\{ u_T \frac{\partial}{\partial n} \ln r + v_T \frac{\partial}{\partial s} \ln r \right\} ds = \Delta U \quad (9)$$

Analogously it can be derived that, for the velocity component  $V = \partial \phi / \partial y$ ,

$$V_\infty = -\frac{1}{2\pi} \int_{\sigma_W} \left\{ v_T \frac{\partial}{\partial n} \ln r - u_T \frac{\partial}{\partial s} \ln r \right\} ds = \Delta V \quad (10)$$

In this way, corrections for the tunnel wall influence in terms of a correction to the freestream velocity and angle of attack are determined by evaluating integrals along the tunnel walls in which the measured disturbance velocities  $u_T$  and  $v_T$  appear. Moreover, as the boundary  $\sigma_M$  does not appear in the ultimate expressions, there is no need to make any assumptions on the actual shape of  $D_M$ . The values of  $\Delta U$  and  $\Delta V$  depend on the choice of the point where Eqs. (9) and (10) are evaluated.

Because the choice of this reference point is more or less arbitrary, a reliable global correction is determined only if the gradients of the wall-induced perturbation field are small; in other words, if there is only a gradual variation of  $\Delta U$  and  $\Delta V$ .

If  $(x_i, y_i)$  denotes the reference point, the actual corrections applied to the measured quantities are defined in a

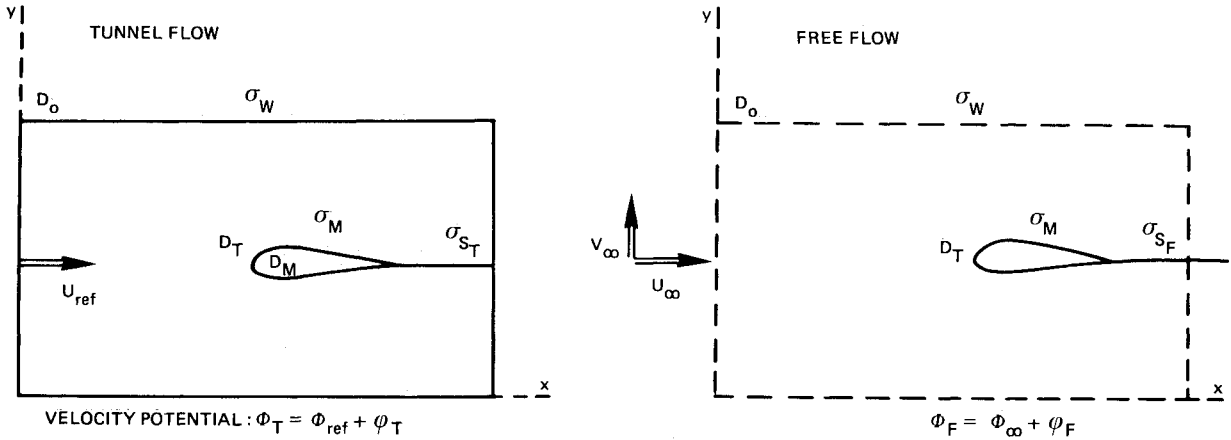


Fig. 1 Flow domains.

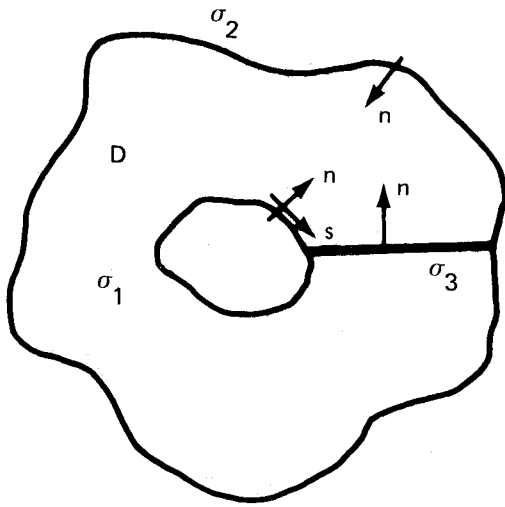


Fig. 2 Flow domain considered for Eq. (1).

more or less classical way as follows:

Incidence:

$$\alpha_C = \alpha_T + \frac{\Delta V}{U_{ref}} \quad (\text{rad}) \quad (11)$$

Dynamic pressure:

$$Q_C = Q_T \left( 1 + 2 \frac{\Delta U}{U_{ref}} \right) \quad (12)$$

Lift:

$$C_{l_C} = C_{l_T} \frac{Q_T}{Q_C} + 2\pi \frac{d}{dx} \left( \frac{\Delta V}{U_{ref}} \right) (x_i - 3/4c) \quad (13)$$

Pressure coefficient:

$$C_{p_C} = C_{p_T} \frac{Q_T}{Q_C} + 2 \frac{\Delta U}{U_{ref}} \quad (14)$$

The applicability of the present method is examined, to some extent, by means of numerical examples in a later section.

#### Local Correction Method

The local correction method, following an approach similar to that of Kraft and Dahm,<sup>3</sup> aims at correcting for

tunnel wall influence in terms of changes in velocity distribution along the model rather than in terms of the onset flow conditions. Again considering the irrotational subsonic flows as depicted in Fig. 1, this means that the undisturbed velocity potentials in both flow situations considered are chosen to be identical, i.e.,

$$\phi_\infty \equiv \phi_{ref} \quad (15)$$

From the condition of tangential flow at the model it follows that, in the tunnel flow,

$$\frac{\partial \phi_T}{\partial n} = \frac{\partial \phi_{ref}}{\partial n} + \frac{\partial \phi_T}{\partial n} = 0 \quad (16)$$

and in free flow,

$$\frac{\partial \phi_F}{\partial n} = \frac{\partial \phi_\infty}{\partial n} + \frac{\partial \phi_F}{\partial n} = \frac{\partial \phi_{ref}}{\partial n} + \frac{\partial \phi_F}{\partial n} = 0 \quad (17)$$

So

$$\frac{\partial \phi_T}{\partial n} = \frac{\partial \phi_F}{\partial n} \quad (18)$$

at the model.

According to Eq. (1), for a point P at the model in tunnel flow, there holds

$$\begin{aligned} \phi_F(P) = \phi_{ref}(P) - \frac{1}{\pi} \int_{\sigma_W} \left\{ \varphi_T \frac{\partial}{\partial n} \ln r - \frac{\partial \phi_T}{\partial n} \ln r \right\} ds \\ - \frac{1}{\pi} \int_{\sigma_M} \left\{ \varphi_T \frac{\partial}{\partial n} \ln r - \frac{\partial \phi_T}{\partial n} \ln r \right\} ds \\ - \frac{1}{\pi} \Delta \phi_T \int_{\sigma_{S_T}} \frac{\partial}{\partial n} \ln r ds \end{aligned} \quad (19)$$

and for a point P at the model in free flow,

$$\begin{aligned} \phi_F(P) = \phi_\infty(P) - \frac{1}{\pi} \int_{\sigma_M} \left\{ \varphi_F \frac{\partial}{\partial n} \ln r - \frac{\partial \phi_F}{\partial n} \ln r \right\} ds \\ - \frac{1}{\pi} \Delta \phi_F \int_{\sigma_{S_F}} \frac{\partial}{\partial n} \ln r ds \end{aligned} \quad (20)$$

Although not really essential, for simplicity it is presumed that the test section is sufficiently long so that the difference between the integrals over  $\sigma_{S_T}$  and  $\sigma_{S_F}$  is negligible. Then,

from subtraction of Eqs. (19) and (20), it follows [with Eqs. (15) and (18)] that

$$\begin{aligned} \varphi_C(P) + \frac{1}{\pi} \int_{\sigma_M} \varphi_C \frac{\partial}{\partial n} \ln r ds + \frac{1}{\pi} \Delta \varphi_C \int_{\sigma_{\hat{T}}} \frac{\partial}{\partial n} \ln r ds \\ = - \frac{1}{\pi} \int_{\sigma_W} \left\{ \varphi_T \frac{\partial}{\partial n} \ln r - \frac{\partial \varphi_T}{\partial n} \ln r \right\} ds \end{aligned} \tag{21}$$

where

$$\varphi_C = \phi_T - \phi_F = \varphi_T - \varphi_F \tag{22}$$

By means of partial integration the term on the right-hand side of Eq. (21) is rewritten as

$$\begin{aligned} - \frac{1}{\pi} \int_{\sigma_W} \left\{ \varphi_T \frac{\partial}{\partial n} \ln r - \frac{\partial \varphi_T}{\partial n} \ln r \right\} ds \\ = - C_{l_T} C - \frac{1}{\pi} \int_{\sigma_W} \left\{ \frac{\partial \varphi_T}{\partial s} \tan^{-1} \frac{y-n}{x-\xi} - \frac{\partial \varphi_T}{\partial n} \ln r \right\} ds \end{aligned} \tag{23}$$

where  $C_{l_T}$  is the measured lift coefficient. Thus, the term on the right-hand side is determined from the measured velocity distribution along the tunnel wall and at the model, and Eq. (21) establishes an integral equation for the correction potential  $\varphi_C$ . Applying the Kutta condition of smooth flow at the trailing edge of the airfoil, this equation is solved by means of a panel method.<sup>2</sup> Differentiation of Eq. (21) establishes the following expression for the tangential

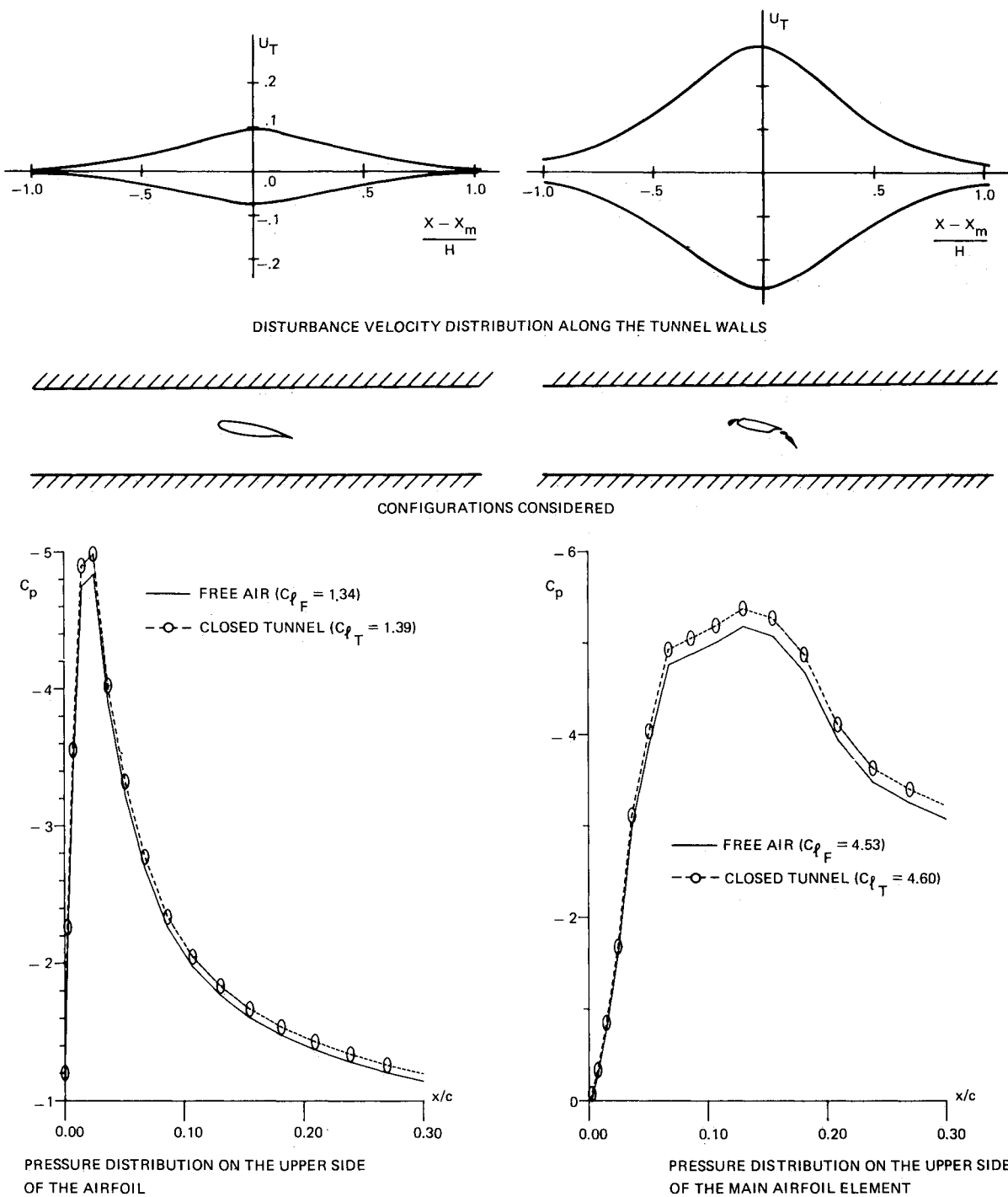


Fig. 3 Numerically simulated flow in free air and closed-wall wind tunnel.

derivative of  $\varphi_C$ :

$$\frac{\partial \varphi_C}{\partial t} = -\frac{1}{\pi} \int_{\sigma_M} \frac{\partial \varphi_C}{\partial s} \frac{\partial}{\partial t} \tan^{-1} \frac{y-\eta}{x-\xi} ds$$

$$-\frac{1}{\pi} \int_{\sigma_W} \left\{ \frac{\partial \varphi_T}{\partial s} \frac{\partial}{\partial t} \tan^{-1} \frac{y-\eta}{x-\xi} - \frac{\partial \varphi_T}{\partial n} \frac{\partial}{\partial t} \ln r \right\} ds \quad (24)$$

Table 1 Globally corrected lift coefficients

	Tunnel		Corrected		Free Air	
	$\alpha_T$	$C_{l_T}$	$\alpha_C$	$C_{l_C}$	$\alpha_F$	$C_{l_F}$
Single airfoil	8.0	1.39	8.11	1.36	8.11	1.36
High-lift configuration	8.0	4.60	8.14	4.51	8.14	4.55

by which a correction to the measured tangential velocity is determined.

In contrast with the previously described (global) method, the present (local) method makes use of detailed information about the model considered. However, whereas the previous method can lead only to an approximation of the free flow, the present method leads to an "exact" description of the free flow within the limits set by the accuracy of measurement and computation. This will be demonstrated by means of numerical examples in the next section.

### Discussion of Results

In order to evaluate the preceding methods with respect to the concepts of global and local correction, a numerical demonstration was performed. To this end, a panel method<sup>2</sup> was applied for the determination of the flow around single and multiple airfoils (see Fig. 3) in a closed-wall wind tunnel as well as in free air. The tunnel walls were located at  $\pm 2$  chords from the airfoil in order to obtain a realistic chord

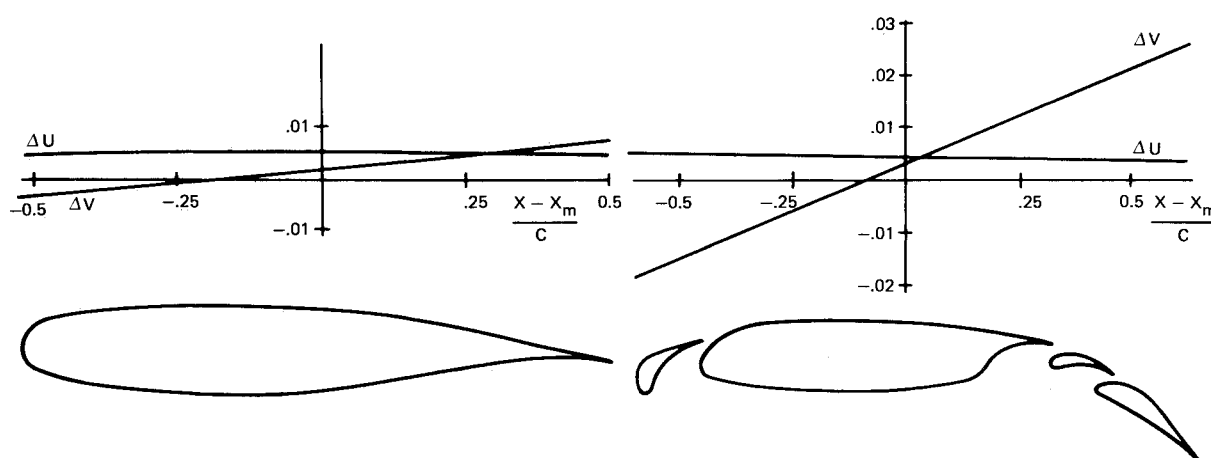


Fig. 4 Distribution of wall interference velocities along the test section centerline.

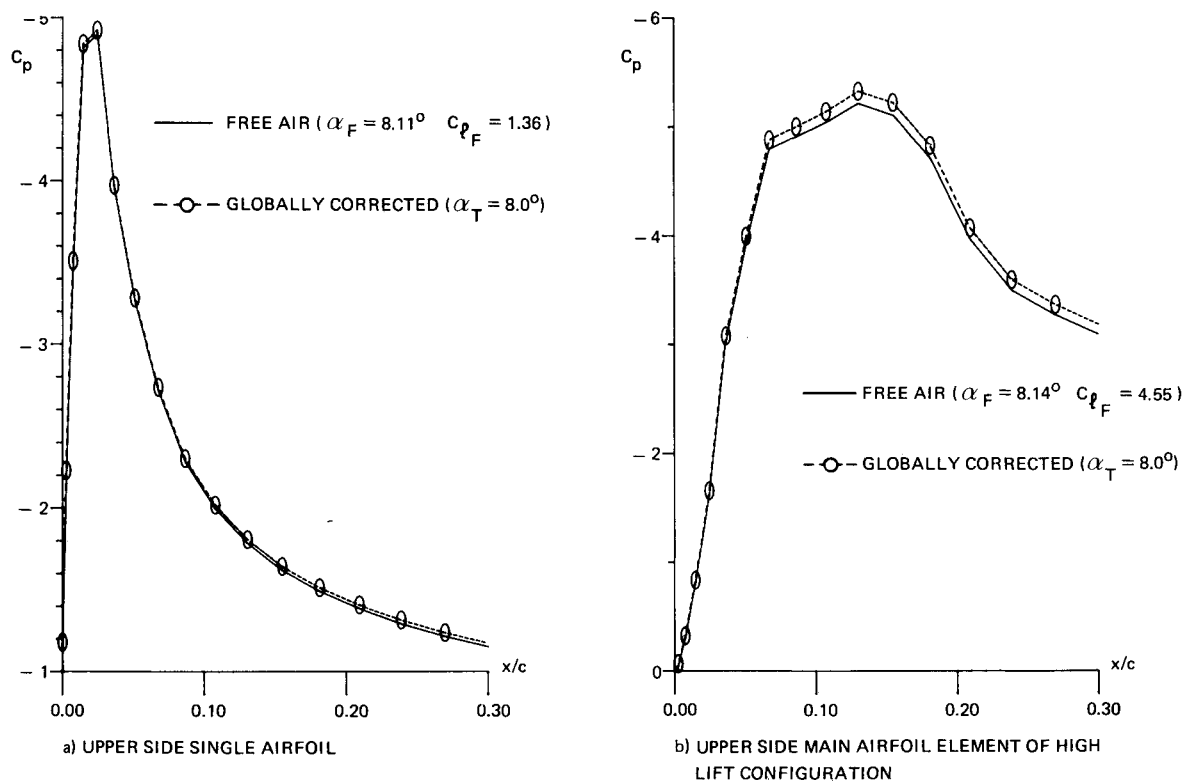


Fig. 5 Globally corrected pressure distributions compared with free-air pressure distributions at the corrected angle of attack.

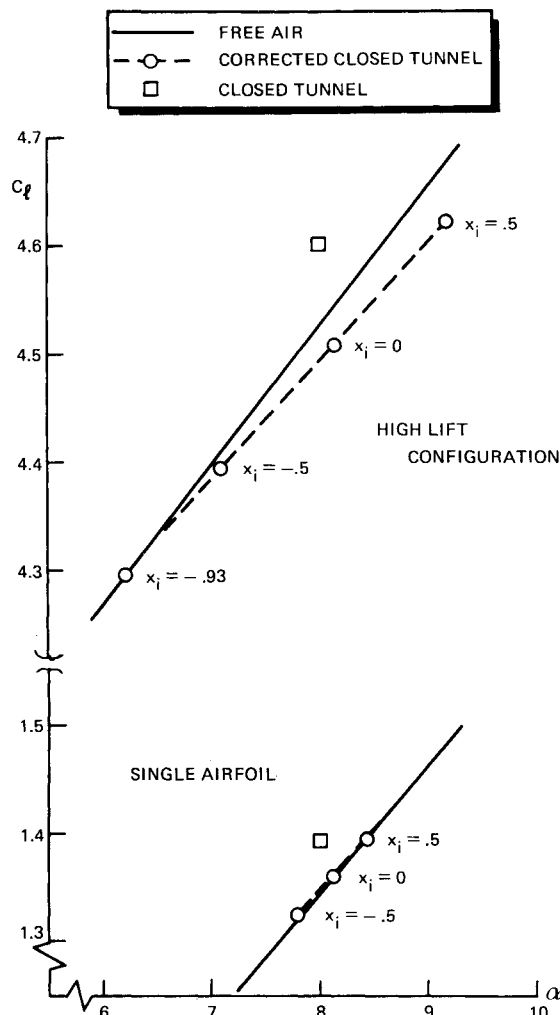


Fig. 6 Globally corrected lift coefficient determined by different choices of the reference point (indicated by  $x_i$ ) compared with the free-air solution.

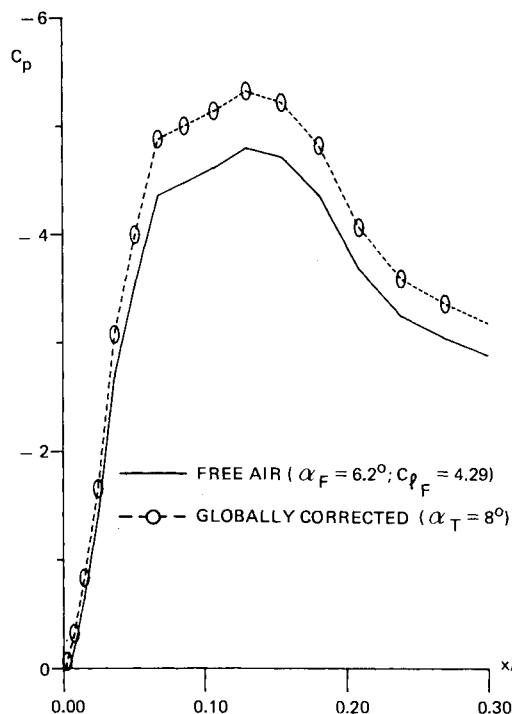


Fig. 7 Globally corrected pressure distribution compared with a free-air pressure distribution which has the same lift coefficient as obtained by means of global correction.

over tunnel height ratio ( $c/H=0.25$ ). As may be seen from Fig. 3, the wall influence on the pressure distribution is of the same order of magnitude in both cases. The “measured” velocity distribution along the tunnel walls (as depicted in Fig. 3) was substituted into Eqs. (9-14) to determine global corrections and Eqs. (21-24) to determine local corrections. With respect to the evaluation of the integrals over  $\sigma_w$  it may be remarked that the integrals over upper and lower walls were determined by using a Gauss-Legendre quadrature formula. The integrals over the front and rear ends were determined analytically by means of a third-order interpolant for the approximation of the velocity components which can be derived from known data at the intersections with the upper and lower walls.<sup>1</sup>

**Global Corrections**

As has been stated previously the tunnel influence corrections determined by means of the global correction method depend on the choice of the reference point where Eqs. (9) and (10) are evaluated; thus the method can be applied successfully only if this choice is of minor importance.

Figure 4 shows the distribution of the wall interference velocities along the test section centerline for both test cases. In both cases the variation of  $\Delta U$  is very small. Therefore, it may be expected that the correction for blockage may be performed equally well in both cases. However, the gradient of the upwash variation is much larger for the high-lift configuration than for the single airfoil.

Choosing the midchord point ( $x_m, y_m$ ) as a reference point for the determination of  $\Delta U$  and  $\Delta V$  the wall corrections have been calculated in terms of a corrected angle of attack and lift coefficient as well as a correct pressure distribution.

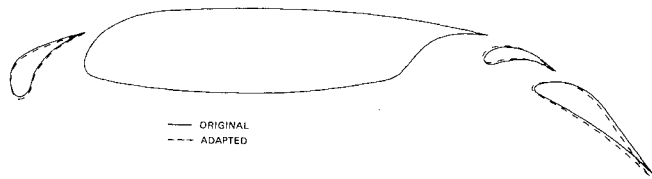


Fig. 8 Model adaptation for simulation of wall interference.

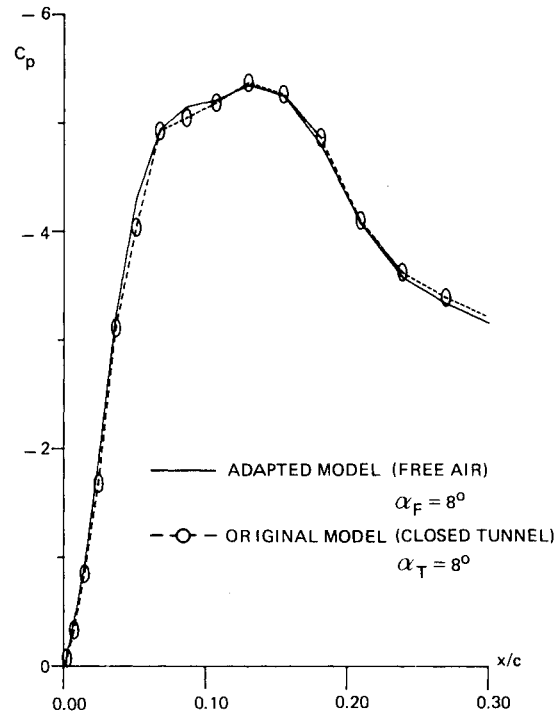


Fig. 9 Pressure distributions on the main element of the adapted configuration in free air and the original configuration in a closed tunnel.

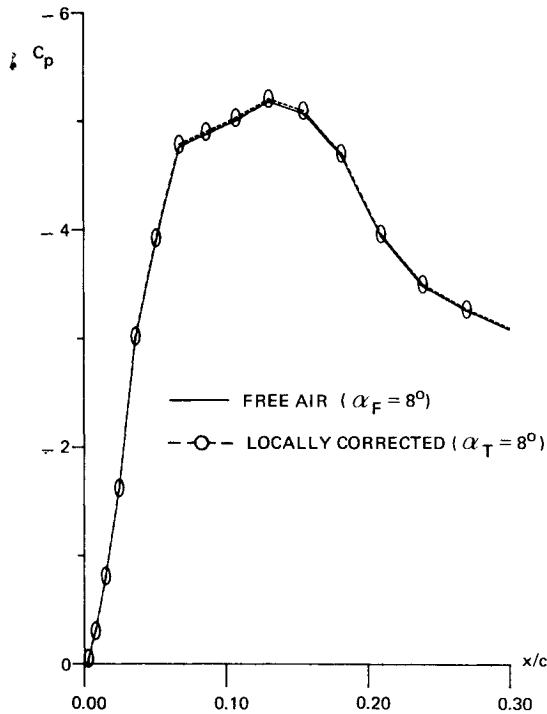


Fig. 10 Locally corrected pressure distribution compared with free-air pressure distribution.

A calculation by means of the panel method for the configuration in free air at the corrected angle of attack provides an easy verification of the correction performed. Table 1 gives a comparison of angle of attack and lift coefficient, while Fig. 5 presents a comparison of the calculated pressure distribution.

From Table 1 it appears that the "free-air solution" obtained by means of global correction is correct for the single airfoil, while Fig. 5 shows that the pressure distribution also is in close agreement with the true solution. As appears from Table 1, the correction for the high-lift configuration, however, is overestimated as far as the total lift coefficient is concerned. The corrections to the pressure distribution are found to be overestimated for the slat and flap and underestimated for the main element (see Fig. 5).

As mentioned previously, the value of the global corrections depends on the reference point location. In order to examine the effect of this choice, different corrected lift coefficients and angles of attack have been determined for different reference point locations. In Fig. 6 the  $C_L$ - $\alpha$  curves thus determined are compared with the free-air solutions. For the single airfoil there is a close agreement between the two curves which implies that the global correction is practically independent of the choice of the reference point. For the high-lift configuration the two curves differ considerably. Their point of intersection corresponds with a reference point located about  $\frac{1}{2}$  chord upstream from the airfoil. Corrections calculated using this point lead to  $\alpha_C = 6.2$  and  $C_{L_C} = 4.29$ .

Although the high-lift configuration in free air has this lift coefficient at this angle of attack, there is only minimal agreement between the globally corrected and free-air pressure distributions, as illustrated in Fig. 7.

Therefore, apparently the high-lift case has to be considered uncorrectable by the global method.

#### Modal Adaptation

The uncorrectability of the high-lift case is obviously due to the large variation of the wall-induced upwash. This part of the wall influence often is interpreted as a virtual

modification of the model camber, which suggests that the agreement between free air and tunnel flow might be improved by modifying the deflection angles of slat, vane, and flap. To investigate this effect a design method for multiple airfoils<sup>2</sup> has been applied. This design method is capable of designing an airfoil such that it will produce, in free air, a specified pressure distribution. The pressure distribution determined for tunnel flow was prescribed as the pressure distribution to be produced by the modified airfoil in free air. In order to keep the interpretation of the results as simple as possible, the design method was applied such that the relative positions of the airfoil elements were modified, while the shape of the elements was kept fixed.

The result of the design process is shown in Fig. 8, where the original and modified configurations are compared. Calculation of the flow around the modified configuration in free air showed that this configuration produces the same lift coefficient as the original configuration in tunnel flow. The pressure distributions, as shown in Fig. 9 for the main element, are, of course, not exactly the same, due to effects that have not been taken into account (e.g., blockage), and because of the limited extent of the modification. However, the camber effect of wall interference is clearly demonstrated. This example shows that strong curvature effects may be interpreted as corrections to slat and flap angles. However, from the point of view of interpretation of wind tunnel measurements this seems rather unattractive. Moreover, determining the corrections requires the use of a design method which makes this procedure particularly unattractive for routine application.

#### Local Corrections

For the present examples it is also possible to eliminate the tunnel wall influence completely from the pressure distribution measured in the tunnel. From the measured velocity distribution along the tunnel walls the correction potential at the airfoil contour is calculated for subsequent correction of the model velocity distribution. The resulting pressure distribution for the main element of the high-lift configuration is presented in Fig. 10. Due to the fact that the example considered here is trivial in the sense that it satisfies all of the underlying assumptions of the present method, the corrected pressure distribution practically coincides with the pressure distribution on the model in free air. The differences that are hardly visible are due to computational imperfections.

#### Concluding Remarks

Two types of wall correction methods (global and local) using measured boundary conditions have been described. The global correction method is by far the most attractive. It does not need any kind of model representation, the computation is very fast because it requires only the evaluation of two integrals, and, moreover, it seems applicable to a wide variety of wind tunnel experiments, two-dimensional as well as three-dimensional.

Generally speaking a global correction method is applicable if the flow around the model in the tunnel is not essentially different from the flow in free air; i.e., if the flow phenomena observed in the tunnel may be considered as free-air flow phenomena but at somewhat different onset flow conditions.

Situations may occur where the difference between the tunnel flow and the free air becomes too large. As has been demonstrated, such a situation is met if the wall-induced upwash variation is too large. Then the determination of a correction simply in terms of angle of attack becomes impossible.

By means of a computational design method it has been shown that the upwash variation may be interpreted as changes in the model geometry. However, this seems a rather inconvenient way of correcting routinely for wall influence.

For the case of large upwash gradients, the application of local corrections seems more satisfactory. For irrotational subsonic flow, such a correction method can be formulated straightforwardly, though at the cost of a detailed representation of the model. The local correction method involves the application of a panel method and, thus, requires much more computation time than the global correction method. But as the application of panel methods is presently a matter of routine, even for three dimensions, this should not be prohibitive. More important is the restriction to irrotational subsonic flow. Moreover, the method is not applicable in transonic flows where nonlinear effects are important.

### References

- <sup>1</sup>Labrujère, T. E., "Correction for Wall Influence by Means of a Measured Boundary Condition Method," National Aerospace Laboratory, Amsterdam, the Netherlands, NLR TR 84114 U, 1984.
- <sup>2</sup>Labrujère, T. E., "MAD, A System for Computer Aided Analysis and Design of Multi-Element Airfoils," National Aerospace Lab, Amsterdam, the Netherlands, NLR TR 83126 U, 1983.
- <sup>3</sup>Kraft, E. M. and Dahm, W. J. A., "Direct Assessment of Wall Interference in a Two Dimensional Subsonic Wind Tunnel," AIAA Paper 82-0187, 1982.
- <sup>4</sup>Ashill, P. R. and Weeks, P. J., "An Experimental Investigation of the Drag of Thick Supercritical Aerofoils," Royal Aircraft Establishment, Clapham, RAE TM (Aero) 1976, 1978.

*From the AIAA Progress in Astronautics and Aeronautics Series...*

## **EXPERIMENTAL DIAGNOSTICS IN GAS PHASE COMBUSTION SYSTEMS—v. 53**

*Editor: Ben T. Zinn; Associate Editors: Craig T. Bowman,  
Daniel L. Hartley, Edward W. Price, and James F. Skifstad*

Our scientific understanding of combustion systems has progressed in the past only as rapidly as penetrating experimental techniques were discovered to clarify the details of the elemental processes of such systems. Prior to 1950, existing understanding about the nature of flame and combustion systems centered in the field of chemical kinetics and thermodynamics. This situation is not surprising since the relatively advanced states of these areas could be directly related to earlier developments by chemists in experimental chemical kinetics. However, modern problems in combustion are not simple ones, and they involve much more than chemistry. The important problems of today often involve nonsteady phenomena, diffusional processes among initially unmixed reactants, and heterogeneous solid-liquid-gas reactions. To clarify the innermost details of such complex systems required the development of new experimental tools. Advances in the development of novel methods have been made steadily during the twenty-five years since 1950, based in large measure on fortuitous advances in the physical sciences occurring at the same time. The diagnostic methods described in this volume—and the methods to be presented in a second volume on combustion experimentation now in preparation—were largely undeveloped a decade ago. These powerful methods make possible a far deeper understanding of the complex processes of combustion than we had thought possible only a short time ago. This book has been planned as a means of disseminating to a wide audience of research and development engineers the techniques that had heretofore been known mainly to specialists.

*Published in 1977, 657 pp., 6 × 9 illus., \$25.00 Mem., \$45.00 List*

**TO ORDER WRITE: Publications Order Dept., AIAA, 1633 Broadway, New York, N.Y. 10019**